Effect of polymer-to-silica ratio on the formation of large three-dimensional cage-like mesostructures†

Rafal M. Grudzien,[a] Bogna E. Grabicka,[a] Maciej Kozak,[b] Stanisław Pikus[c] and Mietek Jaroniec*[a]

Received (in Montpellier, France) 7th March 2006, Accepted 8th May 2006
First published as an Advance Article on the web 2nd June 2006
DOI: 10.1039/b603436e

This work shows the influence of polymer-to-silica ratio on the formation of cage-like ordered mesoporous silica, FDU1, having a three-dimensional face-centered cubic symmetry. The FDU1 samples studied were synthesized from tetraethyl orthosilicate (TEOS) under acidic conditions in the presence of poly(ethylene oxide)–poly(butylene oxide)–poly(ethylene oxide) ($EO_{39}BO_{47}EO_{39}$) triblock copolymer. The molar ratio of triblock copolymer to TEOS in the reaction mixture was varied from 0.0037 to 0.0148. Small angle X-ray scattering, argon adsorption–desorption and high resolution thermogravimetry studies indicate that an optimal $EO_{39}BO_{47}EO_{39}$/TEOS ratio, which led to a high-quality FDU1 material with uniform cage openings, narrow pore size distribution and high specific surface area, was about 0.0074. The FDU1 silicas obtained for lower and higher ratios than the aforementioned value possessed non-uniform cage entrances, broader pore size distributions, lower BET specific surface areas and smaller mesopore diameters.

Introduction

Since discovery of ordered mesoporous silicas (OMSs) with two-dimensional (2-D) channel-like structures, obtained by self-assembly of silica species and ionic surfactants,[1,2] there has been a tremendous interest in their synthesis,[3–6] characterization[7] and applications.[8] OMSs of hexagonal symmetry can be prepared by using ionic surfactants,[3] oligomeric surfactants[9] and non-ionic block copolymers;[4,6,10] especially the use of block copolymers as templates is increasing because of their commercial availability, low-cost and biodegradability.[11]

Further studies in this area led to the development of body-centered cubic (*Im*3*m* symmetry) OMSs with cage-like structure, SBA16,[5,9] where each cage possesses eight connections with other cages. SBA16 was initially synthesized by Zhao *et al.*[4] in the presence of poly(ethylene oxide)–poly(propylene oxide)–poly(ethylene oxide) triblock copolymer Pluronic F127.

Shortly after, FDU1 OMS was reported by Yu and co-workers[6] and further studied by others;[12,13] this material has been prepared by employing more hydrophobic triblock copolymer, poly(ethylene oxide)–poly(butylene oxide)–poly(ethylene oxide),[14] instead of poly(ethylene oxide)–poly (propylene oxide)–poly(ethylene oxide) used for the synthesis of SBA16.[4] It was shown[12] that FDU1 possess a face-centered cubic *Fm*3*m* symmetry with three-dimensional hexagonal intergrowth. Each cage is connected with twelve neighboring pores *via* small apertures to form a multidirectional mesopore network.

In comparison to other polymer-templated cage-like cubic OMSs such as SBA16,[5,9] mesostructured FDU1[6,12] has attracted a lot of attention that originated from its fascinating properties reflected by higher specific surface area, higher pore volume and larger mesopore diameter. Its 3-D structure consisting of cages, where each of them is connected *via* small apertures with twelve neighboring cages, is beneficial for transport of reactants and products, less vulnerable to pore blocking and assures the pore accessibility from any direction. These features make cage-like FDU1[6,12] OMSs very promising materials for applications in adsorption, catalysis, separations and so on.[8]

Matos *et al.*[12] revealed that the size of cage-like pores and their entrances can be controlled by changing time and temperature of the hydrothermal treatment. Later, a new method[15] has been proposed for evaluation of the entrance size in cage-like mesostructures by modification of these OMSs with organosilanes of various lengths to find out the smallest one that is able to block the pore openings. In addition, interesting results[16] were achieved by calcination of FDU1 at different temperatures and boiling in hot water for prolonged periods revealing its extraordinary thermal and hydrothermal stability. More recently, microwave synthesis[17] was reported disclosing a new possibility for short time preparation of FDU1 OMSs. In particular, numerous attempts[18] have been made to meaningfully narrow the pore size distribution and tailor the pore size entrances by addition of inorganic salts under different acid concentrations. Later, it was demonstrated[19] that the synthesis time can be greatly reduced yielding high-quality FDU1 materials.

[a] *Department of Chemistry, Kent State University, Kent, Ohio 44240, USA. E-mail: jaroniec@kent.edu; Fax: 1 330 672 3816; Tel: 1 330 672 3790*
[b] *Department of Macromolecular Physics, A. Mickiewicz University, 61-614 Poznań, Poland*
[c] *Department of Chemistry, Maria Curie-Skłodowska University, 20-031 Lublin, Poland*

† Electronic supplementary information (ESI) available: Structural parameters calculated from the SAXS data (Table S1) and thermogravimetric TG and DTG profiles (Fig. S1 and S2) for the FDU1 samples studied. See DOI: 10.1039/b603436e

The intention of the current work is to study the effect of poly(ethylene oxide)–poly(butylene oxide)–poly(ethylene oxide) triblock copolymer on the formation of three-dimensional cage-like mesoporous materials obtained from tetraethyl orthosilicate under highly acidic conditions. Moreover, this study is not only intended to explore the possibility of controlling the size of cage-like mesopores along with the uniformity of pore entrances but also to find optimal conditions to achieve FDU1 materials with narrow pore size distributions (PSDs) and enlarged pore entrances, *i.e.*, to design more open structures. This is especially advantageous from the viewpoint of utilization of OMSs as hosts for immobilization of various species including biomolecules. Therefore, a series of the FDU1 samples was prepared by varying the copolymer-to-silica ratio. The structural changes and adsorption properties of the aforementioned samples were characterized by small angle X-ray scattering (SAXS), argon adsorption and high resolution thermogravimetry.

Experimental

Materials

Large cage-like FDU1 OMSs were prepared using tetraethyl orthosilicate (TEOS) in the presence of poly(ethylene oxide)–poly(butylene oxide)–poly(ethylene oxide) triblock copolymer ($EO_{39}BO_{47}EO_{39}$; B50-6600, Dow Chemicals) as a structure directing agent under highly acidic conditions. The synthesis mixture composition was analogous to that reported by Yu *et al.*[6] The overall synthesis molar composition was as follows: 1 TEOS : 0.0037–0.0148 B50-6600 : 6 HCl : 155 H_2O. In typical synthesis a specified amount of triblock copolymer (from 0.5 to 4 g) was combined with 120 ml of 2 M HCl under constant stirring for 4 h to form a clear mixture at room temperature. Then, 8.9 ml (8.32 g) of TEOS was added dropwise to B50-6600–HCl solution under vigorous stirring at the same temperature. After further mixing for 6 h, the resulting white precipitate was subsequently heated at 100 °C for another 6 h for hydrothermal treatment. The product was filtered, washed with deionized water and dried in the oven at 80 °C. The as-synthesized nanocomposites were calcined in air at 540 °C for 4 h to remove the template and to make the mesostructure accessible for adsorption. The resulting mesoporous silicas were denoted as FDU1-*x*, where *x* stands for the amount in grams of added triblock copolymer to the synthesis mixture. The $EO_{39}BO_{47}EO_{39}$/TEOS ratio for each FDU1 material is listed in Table 1. For instance, FDU1-2 denotes the sample synthesized by using 2 g of B50-6600 polymer, which for the specified amount of the TEOS used gives the $EO_{39}BO_{47}EO_{39}$/TEOS ratio of 0.0074.

Measurements

Small-angle X-ray scattering (SAXS) measurements were conducted using the NanoSTAR system (Bruker AXS) with pinhole collimation and a two-dimensional detector (HiSTAR), mounted on a micro focus X-ray tube with copper anode and equipped with crossed Göbel mirrors. The sample-to-detector distance was 650 mm. The exposure time for a single frame was 5000–10 000 s. All measurements were performed at room temperature.

Thermogravimetric measurements were carried out under nitrogen atmosphere on a TA Instruments TGA 2950 analyzer using high-resolution mode with maximum heating rate of 5 °C min^{-1}.

Argon and nitrogen adsorption isotherms were measured at −196 °C using both 2010 and 2020 volumetric adsorption analyzers manufactured by Micromeritics, Inc. (Norcross, GA). Before adsorption measurements the samples were outgassed under vacuum for 2 h at 200 °C.

Calculation methods

The BET specific surface area[20] was calculated from adsorption isotherms in the relative pressure range from 0.05 to 0.2. The volumes of small pores (irregular micropores present in the mesopore walls and small apertures interconnecting spherical cages) and mesopores were estimated by integration of the pore size distribution (PSD) in the pore width ranges of 0–4 nm and 4–14 nm, respectively. The single-point total pore volume[20] was estimated from the amount adsorbed at a relative pressure of 0.99. The pore size distribution was calculated from the adsorption branch of isotherms by using the KJS (Kruk, Jaroniec and Sayari) method,[21] which employs the BJH (Barrett, Joyner and Halenda) algorithm for cylindrical pore geometry[22] and the Kelvin-type relation between the pore width and capillary condensation pressure obtained on the basis of adsorption and X-ray diffraction data for high-quality MCM-41 materials. The diameter of ordered (primary) mesopores, w_{KJS}, was defined as the value of pore size at the maximum of PSD; however, because the geometry of primary

Table 1 Measured and calculated parameters for FDU1 silicas studied[a]

Sample	Polymer mass/g^{-1}	Polymer/silica molar ratio	Polymer/silica weight ratio	a/nm	S_{BET}/m^2 g^{-1}	V_c/cc g^{-1}	V_t/cc g^{-1}	w_{KJS}/nm	w_d/nm
FDU1-1	1	0.0037	0.418	23.1	651	0.08[b]	0.62	9.6	—
FDU1-1.5	1.5	0.0055	0.626	23.3	819	0.25	0.72	9.8	13.4
FDU1-2	2	0.0074	0.835	23.3	910	0.29	0.81	10.1	13.5
FDU1-2.5	2.5	0.0093	1.044	23.3	963	0.27	0.98	10.1	14.4
FDU1-3	3	0.0111	1.253	22.9	861	0.23	0.89	9.7	14.1
FDU1-3.5	3.5	0.0129	1.462	22.1	819	0.18	0.97	9.1	14.2
FDU1-4	4	0.0148	1.671	19.2	760	0.03[b]	0.93	7.2	—

[a] Notation: a, unit cell parameter; S_{BET}, BET specific surface area; V_t, single point volume; V_c, volume of complementary pores, which includes irregular micropores and interconnecting apertures below 4 nm; w_{KJS}, mesopore cage diameter; w_d, pore diameter calculated using eqn (1). [b] Volume for pores below 2 nm.

mesopores of FDU1 is spherical, this method leads to a systematic underestimation of the mesopore sizes. Therefore, the mesopore diameters were also estimated by using the relation between the pore width w_d, unit cell parameter a and pore volumes V_p and V_c derived for the *Fm3m* symmetry group:[12]

$$w_d = 0.78a\left(\frac{V_p}{V_p + V_c + 1/\rho}\right)^{1/3} \quad (1)$$

where V_c denotes the volume of complementary small pores, which includes irregular micropores in the mesopore walls and small apertures interconnecting spherical mesopores, and V_p is the volume of ordered spherical mesopores. The pore width w_d was determined by using the unit cell parameter obtained from SAXS data and the pore volumes V_p and V_c estimated by integration of the aforementioned ranges of the PSD curves; the latter were calculated from adsorption branches of the isotherms by the KJS method. The symbol ρ in the above equation denotes the silica density, which was assumed to be 2.2 g cm^{-3}.[21]

Results and discussion

Structural identification

Structural characterization of the calcined FDU1 silicas studied was determined by using SAXS data shown in Fig. 1. As can be seen from this figure the SAXS patterns feature one peak at the scattering vector $\boldsymbol{q}$ = 0.5 that is visible and quite narrow for the FDU1-1, FDU1-1.5, FDU1-2, FDU1-2.5, FDU1-3 samples and it becomes much broader for the FDU1-3.5 and FDU1-4 samples (see the so-called FWHM values, *i.e.*, the values of the full width at half maximum of this peak listed in ESI, Table S1).† In addition to this first reflection the SAXS patterns possess also other peaks, which are the best resolved for the FDU1-2, FDU1-2.5 and FDU1-3 samples. The SAXS patterns for all these samples were assigned according to the face-centered cubic *Fm3m* symmetry analogously as it was done elsewhere for the FDU1 mesostructures.[12] Thus, the observed reflections were indexed as 111, 220, 311, 400, 420 and 600, respectively. The unit cell parameter values calculated for each reflection are similar (see Table 1 and ESI Table S1†) indicting that the assumed symmetry group provides a reasonable representation for the FDU1 mesostructure.

A detailed comparison of the peak intensities for the 220, 311 and 420 reflections present on the SAXS patterns provide some information about structural differences between various samples. This comparison shows that the best structural ordering is observed for the FDU1-2, FDU1-2.5 and FDU1-3 samples. The structural ordering is poor for FDU1-1 and FDU1-1.5 samples and becomes the worst for the FDU1-3.5 and FDU1-4 samples. This finding suggests that the structure deterioration is much more intense when the polymer concentration is too high; this effect is smaller at low polymer concentrations.

Apart from the observed changes in the mesostructural ordering reflected by changes in the peak intensities, one more interesting phenomenon is observed. As can be seen from Fig. 1, the intensity of 220 reflection in relation to 310 peak is rising with the increasing polymer concentration and it becomes the highest for the FDU1-2 (0.0074 ratio) sample, whereas it decreases meaningfully for the FDU1-2.5 and FDU1-3 samples and totally disappears for the FDU1-3.5 and FDU1-4 samples. It is noteworthy that the 220 reflection originates from the lattice plane, which lies on the diagonal of the cubic unit cell face,[12] so its intensity can be related to the entrance size of cage-like mesopores. The aforementioned observation of the changes in the intensity of 220 peak for the samples studied shows that FDU1-2 should have the smallest entrances to the spherical cages in comparison to the other samples, which is confirmed by a delayed desorption and the abrupt closure of the hysteresis loop at the lower limit of relative pressure for argon at −196 °C (see Fig. 2).

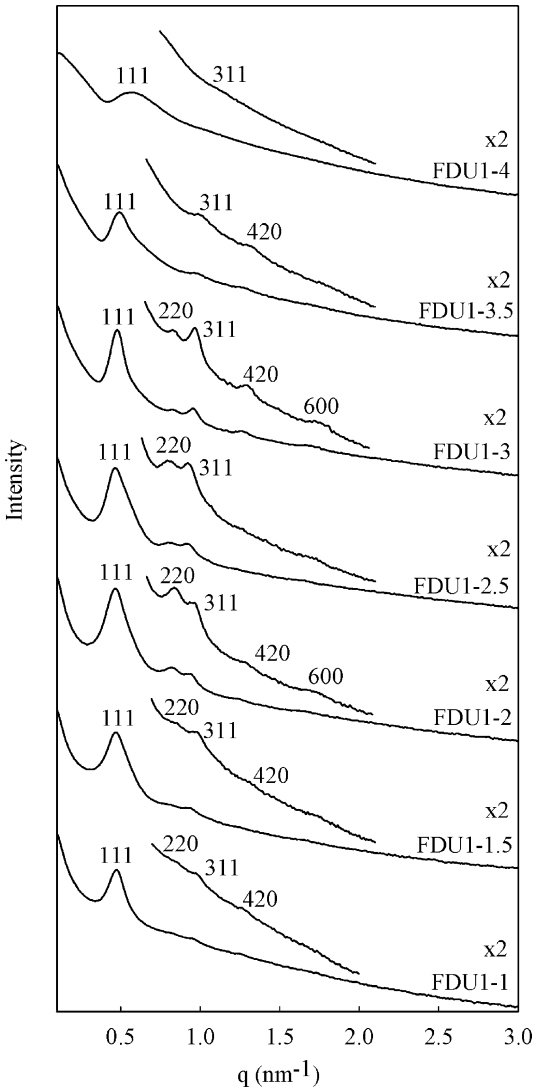

Fig. 1 Small angle X-ray scattering patterns for calcined FDU1 samples synthesized for different triblock copolymer/silica ratios.

Pore structure characterization

Shown in Fig. 2 are argon adsorption–desorption isotherms measured at −196 °C for the FDU1 samples studied; they are

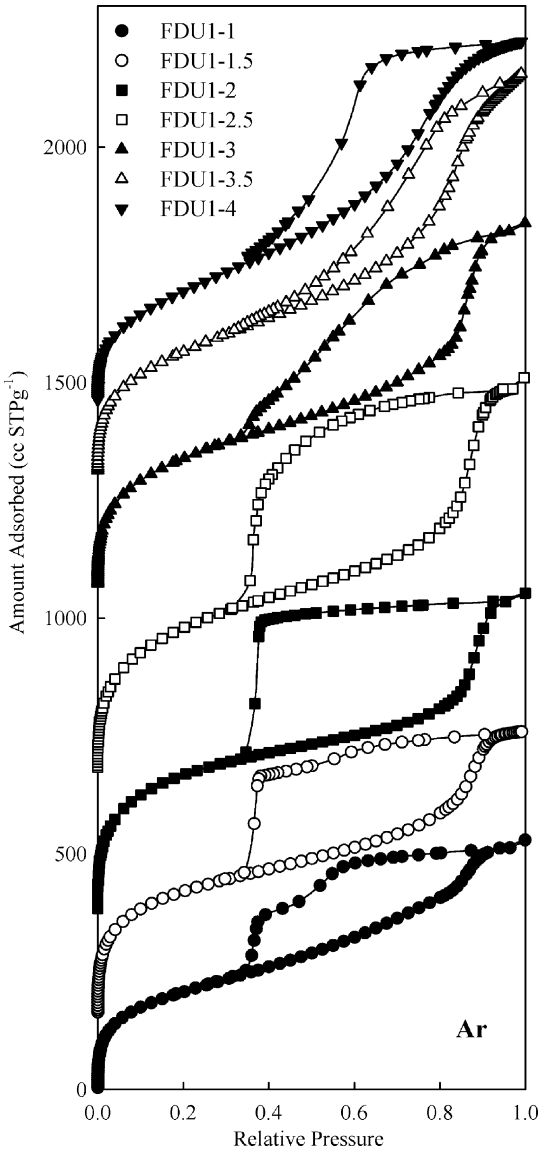

Fig. 2 Argon adsorption–desorption isotherms measured at −196 °C for calcined FDU1 samples synthesized for different triblock copolymer/silica ratios. The isotherms for FDU1-1.5, FDU1-2, FDU1-2.5, FDU1-3, FDU1-3.5 and FDU1-4 were offset vertically by 160, 380, 680, 1070, 1310 and 1460 cc STP g^{-1}, respectively (STP denotes standard temperature and pressure: 273.13 K and 760 mmHg).

type IV[20] with hysteresis loops characteristic for cage-like materials. These isotherms were used to evaluate the BET specific surface area, mesopore diameter, and volumes of complementary and ordered pores, which are listed in Table 1. As can be seen from Table 1 the volume of complementary pores increases with increasing amount of block copolymer, achieving the maximum value for the FDU1-2 sample (which is 0.29 cc g^{-1}) and after that it decreases slowly up to 0.18 cc g^{-1} for FDU1-4.

Shown in Fig. 3 are column charts displaying the evolution of the BET specific surface area (a), volume of ordered mesopores (b) and mesopore width (c) on the polymer amount in the synthesis gel for the OMSs studied. As can be seen from Fig. 3a, the BET surface area for the first sample was 651 m^2 g^{-1} and increased gradually with each additional portion of the polymer added to achieve the maximum value of 963 m^2 g^{-1} for FDU1-2.5; after that value it progressively decreased to reach 760 m^2 g^{-1} for the sample with the highest concentration of polymer. The volume of ordered mesopores (see Fig. 3b) shows a tendency to increase with increasing amount of block copolymer (see Table 1). On the other hand, the pore diameter was not dependent meaningfully on the polymer/silica ratio and was about 10 nm; however at high polymer/silica ratios it was reduced to 7.2 nm. The narrowest pore size distributions (see Fig. 4) are for the samples with the polymer/silica ratios of 0.0074, 0.0093 and 0.0111, whereas PSDs for the remaining samples are much broader.

At higher relative pressures (about 0.8) the adsorption isotherms studied exhibit capillary condensation steps, which are very steep except those for the FDU1-1, FDU1-3.5 and FDU1-4 samples and indicate the presence of uniform mesopores as confirmed by the PSDs curves shown in Fig. 4. For the values of the polymer-to-silica ratio higher than 0.011 and lower than 0.0074, there is a shift of the capillary condensation step towards smaller values of relative pressures that reflects a reduction in the mesopore diameter from ~9.6 and ~9.1 nm (see adsorption isotherms in Fig. 2 and PSDs in Fig. 4 for FDU1-1, FDU1-1.5, FDU1-3.5 and FDU1-4 as well as the pore size values in Table 1). On the other hand, an increase in the polymer-to-silica ratio from 0.0074 to 0.0111 reflects the mesopore enlargement (see PSDs in Fig. 4 for FDU1-2, FDU1-2.5 and FDU1-3 as well as the pore size values in Table 1).

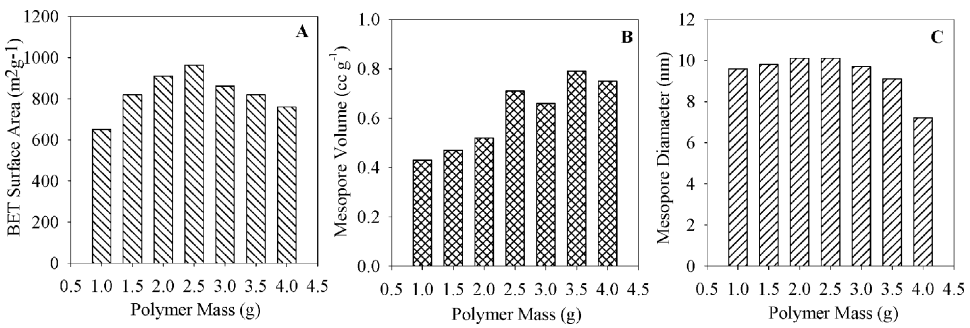

Fig. 3 Evolution of the BET specific surface area (a), volume of ordered mesopores (b) and mesopore cage diameter (c) for the FDU1 silicas synthesized for different triblock copolymer/silica ratios.

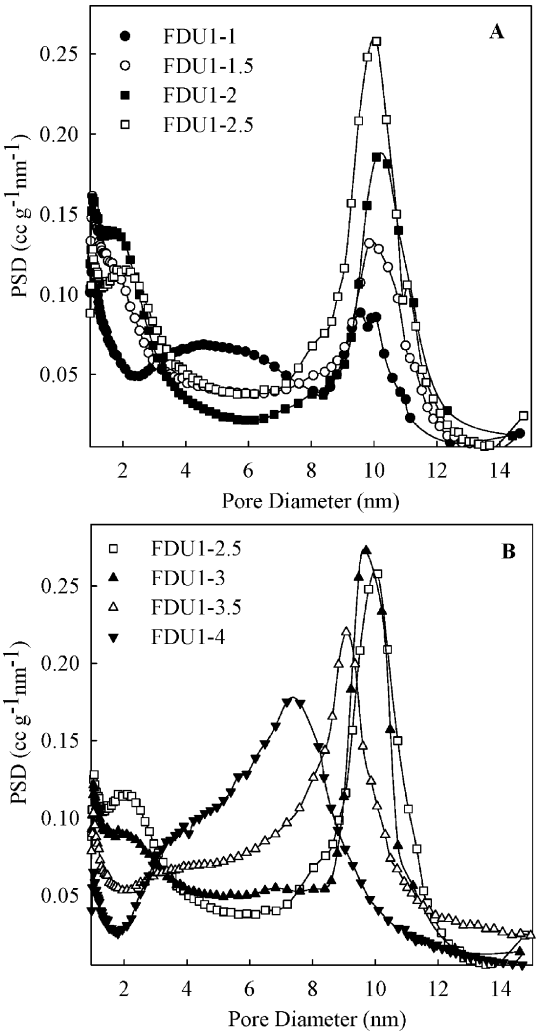

Fig. 4 Pore size distributions (PSDs) calculated according to the KJS method from argon adsorption isotherms for calcined FDU1 samples synthesized for different triblock copolymer/silica ratios.

The shape of hysteresis loop for the samples studied indicates a delay in desorption, which is not surprising because of their cage-like nature. Fig. 2 shows that only adsorption isotherm for the sample with the polymer-to-silica ratio of 0.0074 shows a very steep capillary evaporation step indicating high uniformity of the pore opening sizes. The isotherm curves for the samples with lower ratio than 0.0074 (FDU1-1 and FDU1-1.5) feature two distinct steps on the desorption branch. The first broad step appears somewhere between 0.47–0.6 and the second step is located at a relative pressure of 0.34–0.36, which is the lower limit of the hysteresis loop closure for argon at −196 °C. On the other hand, the isotherm curves for the samples with higher ratio than 0.0074 feature a continuously decreasing desorption branch that reflects a broad distribution of the pore entrance sizes.

The polymer/silica molar ratio for the cage-like FDU1 materials under study was found to be optimal for the value of around 0.0074 that yields a sample with ordered mesopores, narrow pore size distribution and uniform pore entrance sizes, which are at least 4 nm or smaller. Other researchers[7] reported analogous results for silica/surfactant ratios of about 8 : 1 for channel-like MCM-41 materials, speculating about certain stoichiometric reaction between the silica species and ionic alkyltrimethylammonium surfactants. The chain length of surfactants did not influence the silica/surfactant ratio and was approximately constant, equal to ~8. It is noteworthy that the interactions between ionic surfactants and silica are specified as electrostatic interactions. In the case of FDU1 material, interactions between non-ionic triblock copolymer and silica, are less specific and governed by the size and structure of hydrophilic blocks.

The amount of the polymeric template used in the synthesis was determined by high resolution thermogravimetry (TG) as shown in ESI, Fig. S1 and S2.† The TG curves recorded under flowing nitrogen in the range from 100 and 800 °C for the as-synthesized FDU1 materials with progressively increasing amount of the polymeric template (from FDU1-1 to FDU1-4) exhibit a gradual increase in the total weight loss, *i.e.*, 29.13, 37.5, 44.52, 41.56, 49.30, 56.21 and 54.43%, respectively. The differential TG (DTG) profile for a template-containing sample exhibits mainly one sharp peak attributed to the thermodesorption/decomposition of polymer about 275 °C. This temperature is much lower (~200 °C) for the sample with lowest polymer/silica ratio.

Conclusions

Analysis of the SAXS and argon adsorption data shows that cage-like ordered mesoporous FDU1 materials with uniform pore entrances that are smaller than 4 nm as well as large BET specific surface area, high volume of ordered mesopores and narrow pore size distribution are formed for the polymer/silica ratio of about 0.0074. On the other hand, to synthesize FDU1 silica with ordered pores and narrow PSD with substantially enlarged cage openings, the polymer/silica ratio should be maintained in the range from 0.009 to 0.011. The latter materials are expected to be very beneficial for transport of the bulky reactants through cage-like mesopore system as well as for immobilization and encapsulation of various species including biomolecules.

Acknowledgements

M. J. acknowledges support by NSF Grant CHE-0093707. The authors thank Dow Chemicals for providing the triblock copolymer.

References

1 C. T. Kresge, M. E. Leonowicz, W. J. Roth, J. C. Vartuli and J. S. Beck, *Nature*, 1992, **359**, 710.
2 T. Yanagisawa, T. Shimizu, K. Kuroda and C. Kato, *Bull. Chem. Soc. Jpn.*, 1990, **63**, 988.
3 (*a*) M. Kruk, M. Jaroniec and A. Sayari, *Microporous Mesoporous Mater.*, 2000, **35**, 545; (*b*) M. Kruk, M. Jaroniec, M. J. Kim and R. Ryoo, *Langmuir*, 1999, **15**, 5279; (*c*) M. Kruk and M. Jaroniec, *J. Phys. Chem. B*, 1999, **103**, 4590; (*d*) A. Sayari, Y. Yang, M. Kruk and M. Jaroniec, *J. Phys. Chem. B*, 1999, **103**, 1651; (*e*) A. Sayari, M. Kruk and M. Jaroniec, *Catal. Lett.*, 1997, **49**, 147; (*f*) J. R. Matos, L. P. Mercuri, M. Kruk and M. Jaroniec, *Chem. Mater.*, 2001, **13**, 1726.

4 D. Zhao, J. Feng, Q. Huo, N. Melosh, G. H. Frederickson, B. Chmelka and G. D. Stucky, *Science*, 1998, **279**, 548.
5 (*a*) L. Zhao, G. Zhu, D. Zhang, Y. Di, O. Teresaki and Sh. Qiu, *J. Phys. Chem. B*, 2004, **109**, 764; (*b*) Ch.-F. Cheng, Y.-Ch. Lin, H.-H. Cheng, Sh.-M. Liu and H.-Sh. Sheu, *Chem. Lett*., 2004, **33**, 262; (*c*) P. V. D. Voort, M. Benjelloun and E. F. Vansant, *J. Phys. Chem. B*, 2002, **106**, 9027; (*d*) T.-W. Kim, R. Ryoo, M. Kruk, K. P. Gierszal, M. Jaroniec, S. Kamiya and O. Teresaki, *J. Phys. Chem. B*, 2004, **108**, 11480; (*e*) P. I. Ravikovitch and A. V. Neimark, *Langmuir*, 2002, **18**, 9830; (*f*) P. Kipkemboi, A. Fogden, V. Alfredsson and K. Flodstrom, *Langmuir*, 2001, **17**, 5398.
6 C. Yu, Y. Yu and D. Zhao, *Chem. Commun*., 2000, 575.
7 (*a*) M. Jaroniec, M. Kruk, H. J. Shin, R. Ryoo, Y. Sakamoto and O. Teresaki, *Microporous Mesoproous Mater*., 2001, **48**, 127; (*b*) M. Kruk, M. Jaroniec, H. J. Shin and R. Ryoo, *Stud. Surf. Sci. Catal*., 2005, **156**, 55.
8 (*a*) E. Kramer, S. Forster, C. Goltner and M. Antonietti, *Chem. Commun*., 1998, 2287; (*b*) H. Yoshitake, T. Yokoi and T. Tatsumi, *Chem. Lett*., 2002, 586; (*c*) J. Deere, E. Magner, J. G. Wall and B. K. Hodnett, *Chem. Commun*., 2001, 46510; (*d*) S. Kang, J. S. Yu, M. Kruk and M. Jaroniec, *Chem. Commun*., 2002, 1670; (*e*) J. Deer, E. Magner, J. G. Wall and B. K. Hodnett, *Chem. Commun*., 2001, 465; (*f*) Y.-J. Han, J. T. Watson, G. D. Stucky and A. Butler, *J. Mol. Catal. B: Enzym*., 2002, **17**, 1.
9 L. Wang, J. Fan, B. Tian, H. Yang, CH. Yu, B. Tu and D. Zhao, *Microporous Mesoporous Mater*., 2004, **67**, 135.
10 P. F. Fulvio and M. Jaroniec, *Stud. Surf. Sci. Catal*., 2005, **156**, 78.
11 N. Kumar, M. N. V. Majeti and A. J. Domb, *Adv. Drug Delivery Rev*., 2001, **53**, 23.
12 J. R. Matos, M. Kruk, L. P. Mercuri, M. Jaroniec, L. Zhao, T. Kamiyama, O. Teresaki, T. J. Pinnavaia and Y. Liu, *J. Am. Chem. Soc*., 2003, **125**, 821.
13 J. R. Matos, L. P. Mercuri, M. Kruk and M. Jaroniec, *Langmuir*, 2002, **18**, 884.
14 Y. A. I. Abu-Lebdeh, P. M. Budd and V. M. Nace, *J. Mater. Chem*., 1998, **8**, 1839.
15 M. Kruk, V. Antochshuk, J. R. Matos, L. P. Mercuri and M. Jaroniec, *J. Am. Chem. Soc*., 2002, **124**, 168.
16 M. Kruk, E. B. Celer and M. Jaroniec, *Chem. Mater*., 2004, **16**, 698.
17 (*a*) M. C. A. Fantini, J. R. Matos, L. C. Cides da Silva, L. P. Mercuri, G. O. Chiercei, E. B. Celer and M. Jaroniec, *Mater. Sci. Eng., B*, 2004, **112**, 106; (*b*) L. C. Cides da Silva, G. Abate, N. Andrea, M. C. A. Fantini, J. C. Masini, L. P. Mercuri, O. Olkhovyk, M. Jaroniec and J. R. Matos, *Stud. Surf. Sci. Catal*., 2005, **156**, 941.
18 (*a*) M. Kruk, E. B. Celer, J. R. Matos, S. Pikus and M. Jaroniec, *J. Phys. Chem. B*, 2005, **109**, 3838; (*b*) R. M. Grudzien and M. Jaroniec, *Chem. Commun*., 2005, 1076.
19 R. M. Grudzien and M. Jaroniec, *Stud. Surf. Sci. Catal*., 2005, **156**, 105.
20 K. S. Sing, D. H. Everett, R. A. W. Haul, L. Moscou, R. A. Pierotti, J. Rouquerol and T. Siemieniewska, *Pure Appl. Chem*., 1985, **57**, 603.
21 M. Kruk, M. Jaroniec and A. Sayari, *Langmuir*, 1997, **13**, 6267.
22 E. P. Barrett, L. G. Joyner and P. P. Halenda, *J. Am. Chem. Soc*., 1951, **73**, 373.

